Journal of Magnetic Resonance 207 (2010) 287–293

Contents lists available at ScienceDirect

Journal of Magnetic Resonance

journal homepage: www.elsevier.com/locate/jmr

Hydration water dynamics in biopolymers from NMR relaxation in the rotating frame

Barbara Blicharska [a,*], Hartwig Peemoeller [b], Magdalena Witek [a]

[a] Institute of Physics, Jagiellonian University, Kraków, Poland
[b] Department of Physics and Astronomy, University of Waterloo, Canada

ARTICLE INFO

Article history:
Received 2 June 2010
Revised 13 September 2010
Available online 24 September 2010

Keywords:
NMR relaxation
$T_{1\rho}$ dispersion profile
Biopolymers

ABSTRACT

Assuming dipole–dipole interaction as the dominant relaxation mechanism of protons of water molecules adsorbed onto macromolecule (biopolymer) surfaces we have been able to model the dependences of relaxation rates on temperature and frequency. For adsorbed water molecules the correlation times are of the order of 10^{-5} s, for which the dispersion region of spin–lattice relaxation rates in the rotating frame $R_{1\rho} = 1/T_{1\rho}$ appears over a range of easily accessible B_1 values. Measurements of $T_{1\rho}$ at constant temperature and different B_1 values then give the "dispersion profiles" for biopolymers. Fitting a theoretical relaxation model to these profiles allows for the estimation of correlation times. This way of obtaining the correlation time is easier and faster than approaches involving measurements of the temperature dependence of $R_1 = 1/T_1$. The $T_{1\rho}$ dispersion approach, as a tool for molecular dynamics study, has been demonstrated for several hydrated biopolymer systems including crystalline cellulose, starch of different origins (potato, corn, oat, wheat), paper (modern, old) and lyophilized proteins (albumin, lysozyme).

1. Introduction

NMR relaxation times and their dependence on temperature and magnetic field have proved to be a useful source of information about molecular dynamics of water adsorbed on biopolymer surfaces and functional groups of biopolymers [1]. Many studies of spin–lattice relaxation time in the laboratory frame, T_1, spin–spin relaxation time, T_2 and spin–lattice relaxation time in the rotating frame, $T_{1\rho}$, of different biopolymers have been reported in the literature [2–10]. For example, the molecular origin of nuclear spin relaxation has been examined in cellulose and its derivatives [4–6]. The effect of temperature on nuclear spin relaxation has been probed extensively in biopolymers in cell walls [7–9] in order to understand the behavior of main functional groups. Starch chain dynamics has been studied by means of the temperature dependence of relaxation times in order to investigate structure–hydration relationships [11,12].

$T_{1\rho}$ has been shown to be sensitive to chemical exchange between water and protein protons [13,14], to exchange of hydration water [15] and to susceptibility effects [16]. The slowing down of the inherent motion of proteins in solution by denaturation or cross-linking can enhance nuclear spin relaxation dramatically and modifies the shape of the relaxation dispersion curve. These effects have been exploited in NMR studies of molecular dynamics aspects in protein solutions [14,15,17].

The MRI contrast afforded by $T_{1\rho}$ has been shown to offer unique information about physical disorders [13,18]. The physical properties of blood and of other tissue environments have been studied through measurements of dispersion (B_1 dependence) of spin–lattice relaxation rates in the rotating frame $R_{1\rho} = 1/T_{1\rho}$ [18,19].

The measurement of proton $T_{1\rho}$ offers an excellent way of probing the molecular motions characterized by frequencies in the mid-kHz region, typically observed for the main chain segmental motions of polymers above the glass transition temperature and for the dynamics of hydration water adsorbed by polymers. The interpretation of the temperature and field dependence of relaxation data, however, still raises questions about a model for molecular dynamics of adsorbed water in biopolymer systems.

In this paper we report on measurements of dispersion of $R_{1\rho}$ for different biopolymers: cellulose, starch, lyophilized powders of albumin and lysozyme and paper samples. A basis of data interpretation is a model of intra-molecular dipole–dipole interactions between protons of adsorbed water molecules. It allows for calculation of the correlation time τ, the primary parameter describing local dynamics in polymer–water systems. Correlation times characteristic of water adsorbed onto polymers and biomacromolecules are long compared to those in bulk water [2,3,20] and values in the microsecond range have been reported [21,22]. A particular value reflects details about dynamics of water and polymers

* Corresponding author. Address: Institute of Physics, Jagiellonian University, Reymonta 4, 30 059 Kraków, Poland. Fax: +48 12 634 2038.
E-mail address: BB@netmail.if.uj.edu.pl (B. Blicharska).

1090-7807/$ - see front matter © 2010 Elsevier Inc. All rights reserved.
doi:10.1016/j.jmr.2010.09.012

as well as about water–biopolymer interactions. In addition, the activation energy E can be derived from the temperature dependence of correlation times, estimated from dispersion profiles measured at different temperatures. Knowledge of both τ and E may be helpful in providing a better explanation, than presently available, of differences in molecular dynamics of water molecules adsorbed onto the surfaces of different biopolymers.

2. Materials and methods

2.1. Samples of biopolymers

Samples of powdered cellulose (Sigma-Aldrich, Poznań, Poland) and potato starch (Nowamyl, Łobez, Polska), corn and wheat starch (Kröner Staerke GmbH&Co. Ibbenburen, Germany) and oat starch (Alko Ltd. Rajamaki, Finland) were used without further treatment as hydrated powders and suspensions in distilled water. The moisture contents (MC) were 13%, 7% and 8% for potato, oat, corn and wheat starch powder, respectively. The samples of lyophilized powders of albumin, lysozyme and haemoglobin were kept at laboratory humidity and temperature and their moisture contents were (10 ± 2)%. Three types of paper (modern, old, "Swiecie" type) of and cotton threads of MC ~10% each were also used in this study.

2.2. NMR relaxation methods

Proton NMR relaxation time measurements were performed on a Minispec Bruker spectrometer working at a resonant frequency of 60 MHz. The Inversion Recovery (IR) and the standard spin-locking pulse sequences were used to measure T_1 and $T_{1\rho}$, respectively. The length of the $\pi/2$ pulse was 2 μs. Delay (TI) between pulses in the IR sequence was in the range 10–2000 ms, changing as a geometrical progression. Typically, 12–24 values of TI were used. The recycle delay in the IR sequence was not shorter than 2 s, depending on sample. All T_1 measurements were repeated at least six times. For $T_{1\rho}$, typically 8–16 spin-locking delays were used in the range of 0.1–4 ms. By changing the attenuation of the locking pulse from 15 dB to 40 dB, the field B_1 was changed from 0.3×10^{-4} T to 40×10^{-4} T and a minimum of 10 points were collected in each experiment. The magnitude of B_1 was adjusted by finding the first maximum of the FID after a $\pi/2$ pulse of length $\pi/2\gamma B_1$. The $T_{1\rho}$ measurements for starch were performed over the temperature range of 8–55 °C. The sample temperature was defined with an accuracy of ±1 °C.

All relaxation time values were obtained by fitting a multiexponential function to the decay/recovery data using a Levenburg–Marquardt non-linear curve-fitting routine. Single exponential recovery curves were observed for T_1 measurements and up to two relaxation components for $T_{1\rho}$ measurements.

2.3. Relaxation model description

Assumption of intra-molecular dipolar interaction and isotropic motion leads to the well-known formulae for relaxation rates [23] of a pair of protons with constant inter-proton distance r:

- for spin–lattice and spin–spin relaxation

$$R_1 = \frac{1}{T_1} = 2A\left(\frac{\tau}{1+\omega^2\tau^2} + \frac{4\tau}{1+4\omega^2\tau^2}\right), \quad (1)$$

$$R_2 = \frac{1}{T_2} = A\left(3\tau + \frac{5\tau}{1+\omega^2\tau^2} + \frac{2\tau}{1+4\omega^2\tau^2}\right), \quad (2)$$

- for spin–lattice relaxation in the rotating frame with $\omega_1 = \gamma B_1$

$$R_{1\rho} = \frac{1}{T_{1\rho}} = A\left(\frac{3\tau}{1+4\omega_1^2\tau^2} + \frac{5\tau}{1+\omega^2\tau^2} + \frac{2\tau}{1+4\omega^2\tau^2}\right), \quad (3)$$

where $\omega = \gamma B_0$ is the proton resonant frequency, constant $A = \frac{3}{20}\gamma^4\hbar^2\left(\frac{\mu_0}{4\pi}\right)^2 r^{-6}$ and τ is the correlation time, depending on temperature according to the Arrhenius law $\tau = \tau_o e^{-\frac{E}{kT}}$.

Simulations of the above relaxation rates as a function of correlation times ranging from 10^{-12} s to 1 s at resonant frequencies for protons have shown that in comparison to relaxation rates R_1, which start to be frequency dependent as correlation times exceed about 10^{-9} s, the relaxation rates $R_{1\rho}$ show dependence on ω_1 at much longer correlation times, of the order of 10^{-2} s [1,24]. This means that $R_{1\rho}$ dispersion measurements are more sensitive than R_1 dispersion measurements to slow molecular motions, which are characteristic of dynamics of water molecules adsorbed onto the surface of biopolymers [2,3]. Another advantage of $R_{1\rho}$ measurements is that we are able to vary the B_1 value relatively easily by changing the spin-locking pulse amplitude through attenuation of the rf pulse. This procedure for measuring relaxation dispersion is much simpler than changing the strength of the stabilized magnetic field B_0. While the minimum value of B_0 in fast field cycling relaxometry methods is limited to the value of the earth's magnetic field, using rotating frame dispersion it is possible to use smaller fields $B_1 \sim 10^{-5}$ T [10,25].

For slow motions satisfying $\omega^2\tau^2 \gg 1$, the first term of the Eq. (3) is much larger than the last two terms. At constant B_0 and temperature (i.e. constant correlation time) Eq. (3) can be written as:

$$R_{1\rho} = a + \frac{b}{1+4\omega_1^2\tau^2}, \quad (4)$$

where a and b are constants. Fitting Eq. (4) to the experimental data (dispersion profile) allows us to evaluate τ.

Fig. 1 shows the simulations of dispersion profiles Eq. (4) for τ ranging from 6×10^{-7} s to 1.9×10^{-4} s. If τ is outside of this range practically no dispersion is observed. This means that using this method one can evaluate the correlation times over the range 6×10^{-7}–2×10^{-4} s.

A comment about the use of a single correlation time model is in order. In the derivation of Eqs. (1)–(3) an exponential correlation function is assumed, which leads to the Debye type spectral density functions with single correlation time, appearing in these equations. In general, the water molecule dynamics in hydrated biopolymers is expected to be more complicated. Non-exponential correlation functions, leading to non-Debye type spectral density

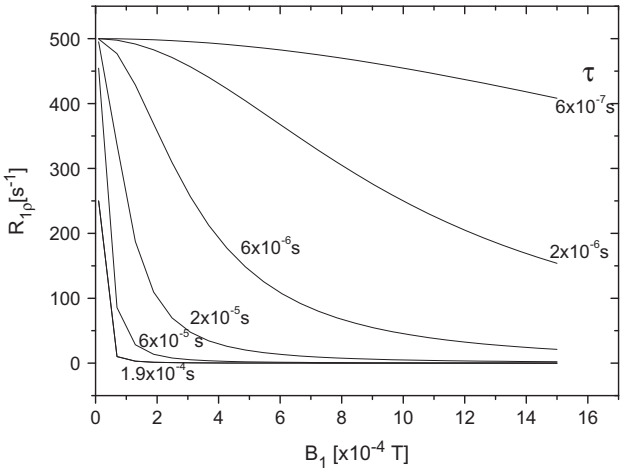

Fig. 1. Simulation of dispersion profiles Eq. (4) for different values of correlation time τ.

functions involving distributions of correlation times, have been applied to a number of related systems(e.g., [20,22]). In addition, considering that an important part of the hydration process in these hydrophilic biopolymers involves formation of hydrogen bonds between the water and the surface, anisotropic water molecule motion may be involved [26]. In the samples considered in the present study Eq. (4), which is derived from Eq. (3), was found to provide a good fit to the rotating frame dispersion curves. The $R_{1\rho}$ dispersion experiment is sensitive to motions with frequencies in the ω_1 range. The fact that Eq. (4) satisfactorily describes a major dispersion step in the present data sets indicates that motions with this correlation time, or perhaps with correlation times spread over a narrow distribution centered about this correlation time, play an important role in characterizing the dynamics. We consider the correlation times obtained from the $R_{1\rho}$ dispersion experiments to be effective correlation times, which provide us with a time scale for an important component of hydration water dynamics.

3. Results and discussion

Water in biopolymers exist in at least two different environments [2–4]. The actual number of water fractions depends on the moisture content. In addition to bulk-like water present in biopolymer suspension, some authors distinguish two or three types of water associated with the micro-structure of the biopolymer called "freezable" and "non-freezable" water [27]. In our case, due to a long spectrometer dead time (>20 μs), the rapidly decaying solid-like FID signal was not visible.

The $T_{1\rho}$ decay curves of the samples with smaller MC were well described by the sum of two exponential components; a "slow" component and a "fast" component decaying with long and short $T_{1\rho}$, respectively. The fast component usually had a smaller amplitude and was either slightly dependent on temperature and frequency or not at all. Typical examples of the $T_{1\rho}$ dispersion behavior and temperature dependence of the two $T_{1\rho}$ components in the low hydration native starch powder sample are given in Figs. 2 and 3, respectively. The solid line in Fig. 2 was calculated from Eq. (4) using the best fit parameters a, b and τ given on the figure, which were obtained from a least-squares fit of Eq. (4) to the data. In the final analysis the data for the fast component was not sufficiently well defined to obtain information on molecular dynamics of water molecules associated with this component.

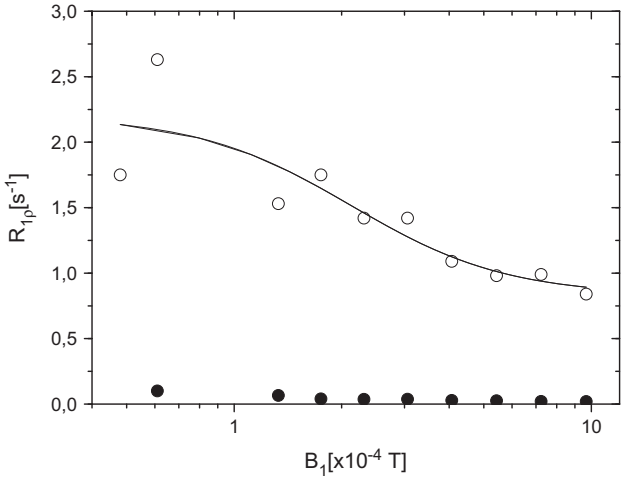

Fig. 2. $R_{1\rho}$ dispersion profiles for the two components observed in native potato starch powder at laboratory humidity (MC = 13%) and temperature of 25 °C. The solid line was calculated using Eq. (4) with the following parameters $a = (0.83 \pm 0.22)\ s^{-1}$, $b = (1.4 \pm 0.2)\ s^{-1}$ and $\tau = (0.87 \pm 0.79) \times 10^{-5}$ s.

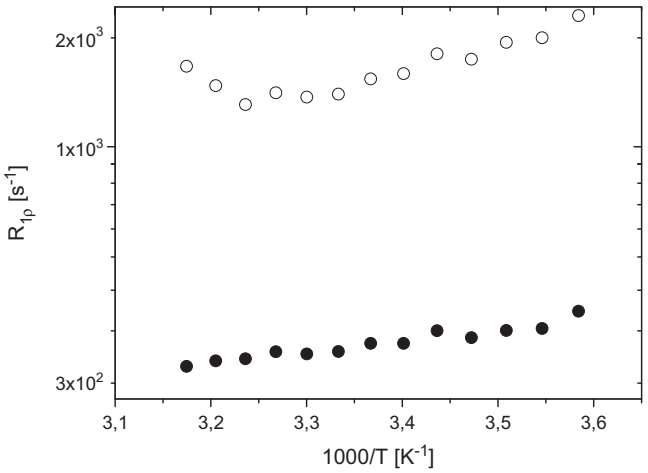

Fig. 3. Temperature dependence of the fast (open circle) and slow (closed circles) components of $R_{1\rho}$ for native potato starch powder at room humidity (MC = 13%) and $B_1 = 1.36 \times 10^{-4}$ T.

Thus, in this study we considered only the component with longer $T_{1\rho}$. In other samples, mostly in water suspensions samples, only single (longer) exponential decay was observed.

The observed water proton relaxation behavior can also be influenced by exchange of magnetization between different water fractions. Evidence for this exchange may be the observation of a single T_1, while two components of T_2 and $T_{1\rho}$ have been discerned. In order to analyze the observed results for exchange it is important to have available reasonably complete information about the apparent relaxation parameters. In the present report the slow component is well defined. However, the fast component (magnetization fraction and relaxation time) is relatively poorly defined, precluding a detailed exchange analysis without additional information.

If exchange is present, and if $T_{1\rho}$ is dispersive, with Eq. (4) providing a reasonable description of the dispersion step, the derived correlation time still must relate to motion of proton internuclear vectors in the sample. The precise details of the dispersion step will be a function of the sizes of the spin groups involved, their relaxation rates and the exchange rates, however, the correlation time derived from the dispersion via Eq. (4) will be indicative of dynamics on the time scale of such correlation time. Also, the correlation times so derived are not representative of the time scale of the exchange motion itself. This can be seen by noting that if the slow correlation time (~20 μs), derived from the $T_{1\rho}$ dispersion data, were associated with the exchange process itself then: (a) it would be fast enough to drive the systems being studied into the fast exchange regime (single exponential relaxation behavior) and (b) it would not be expected to remain constant as the sample stoichiometry and moisture content vary considerably. For example, Fig. 4 shows the comparison of the dispersion profiles obtained for two very different types of samples: lysozyme powder and old paper at room temperature. The model described by Eq. (4) was fitted to the experimental data for both types of samples. There are substantial compositional and structural differences between these two types of samples and therefore the $R_{1\rho}$ values are also distinct. However, the assumed model works for both samples, yielding correlation times that are equal within the experimental error. For simplicity we neglect effects of exchange in the following analysis of the $T_{1\rho}$ results.

Fig. 5 shows the $R_{1\rho}$ dispersion profiles, constructed using the data presented in [4] for hydrated cellulose at moisture contents of 49.9% and 218%, measured at a proton resonant frequency of 17.1 MHz and at 25 °C. Eq. (4) was fitted ($R^2 = 0.99$) to the data

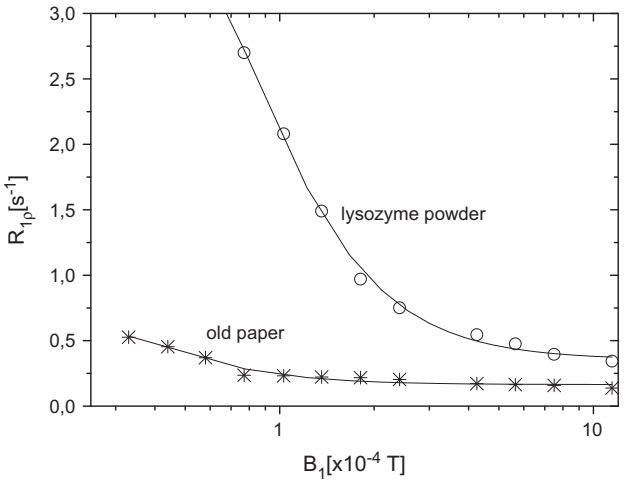

Fig. 4. Dispersion profiles of $R_{1\rho}$ for samples of lysozyme powder and old paper. The solid lines were calculated from Eq. (4) with the following best fit parameters: lysozyme: $a = (0.354 \pm 0.028)\ s^{-1}$, $b = (5.0 \pm 0.5)\ s^{-1}$, $\tau = (2.57 \pm 1.05) \times 10^{-5}$ s; old paper: $a = (0.164 \pm 0.015)\ s^{-1}$, $b = (0.69 \pm 0.16)\ s^{-1}$, $\tau = (5.27 \pm 3.46) \times 10^{-5}$ s.

and the best fit τ values are $(1.1 \pm 0.1) \times 10^{-5}$ s and $(1.3 \pm 0.4) \times 10^{-5}$ s for the samples of MC = 49.9% (Fig. 5a) and MC = 218% (Fig. 5b), respectively. These results suggest that for a particular type of polymer the τ for the slow water is not very sensitive to the degree of hydration.

Correlation times estimated by fitting Eq. (4) to $R_{1\rho}$ dispersion profiles obtained in this study for samples of cellulose with MC above 100% (suspension) and MC = 15% (room humidity) are presented in Table 1. Values of correlation times do not depend significantly on MC or on type of hydration (suspension in water or air hydration). However, the T_1 values are almost three times longer for the suspension than for the powder sample. In addition, values of $T_{1\rho}$ at all B_1 values are considerably longer in the suspensions. These results are consistent with the following interpretation. At a hydration level of 15% all water in the sample is closely associated with the polymer and has the characteristic slow dynamics component with τ in the 10^{-5} s range. As a consequence of this slow motion the proton $T_{1\rho}$ rate exhibits a large dispersion step. At the same time, hydration water dynamics contains nanosecond scale motion, which reduces proton T_1 from 3 s in bulk water to T_1 of the order of 100 ms in low hydration polymer samples. As the hydration level is increased to MC > 100% this water retains its slow dynamics both on the 10^{-5} s and nanosecond time scales. The remaining water at this higher hydration level is not closely associated with the polymer and undergoes relatively fast motion with the result that its proton $T_{1\rho}$ and T_1 relaxation rates are relatively small – closer to the bulk water values. Due to fast exchange between these two water phases on the T_1 time scales only single component recovery curves are observed at MC > 100% and the resulting observed, average relaxation rate is considerably smaller than the corresponding rate at 15% moisture content. Although on the $T_{1\rho}$ time scale exchange between the above two water phases is not in the fast exchange regime, it is effective enough to yield only a poorly defined short $T_{1\rho}$ component and a main component with a $T_{1\rho}$ rate that nearly equals the weighted average of the relaxation rates of the two phases. As such, this component $T_{1\rho}$ rate has a considerably smaller dispersion step with similar τ as seen in the low hydration samples.

In order to gain additional insight into molecular dynamics in these very different polymers further $R_{1\rho}$ dispersion profiles were measured at room temperature for other samples, such as starch of different origin, paper and lyophilized protein powders. The τ values derived from the dispersion profiles for starch powder of different origin at 25 °C, at laboratory humidity, are presented in Table 1. To facilitate the interpretation of the data, T_1 have been measured also (Table 1). Potato starch has a different molecular and micro-structure than cereal starches (corn, oat and wheat) [28–30]. Among cereal starches corn starch is characterized by a special type of arrangement of carbohydrate chains, which are combined with lipids (V-type) [31,32]. These characteristics of a given type of starch determine the space accessible to water, amount of water that can adsorb and can interact within carbohydrate chains and the overall dynamics of carbohydrate chains. In turn, these aspects can be reflected in the T_1 values (Table 1). For example, relative to the other starches, potato starch is characterized by the most open micro-structure which is more easily accessible to water and results in the shortest T_1 values. No significant differences can be seen in correlation times between samples, which indicates similar interaction and local dynamics at the starch–water interface.

Table 1 shows also values of T_1 and τ for different paper samples. In our previous investigations, based on T_1, we found that the ageing of paper changes (shortens) the relaxation times, as a result of the crystallization process of cellulose [33]. Here we observe the shortening of correlation times, which may relate to differences in the polymer micro-structure of paper, which in turn is also connected with paper quality (longevity).

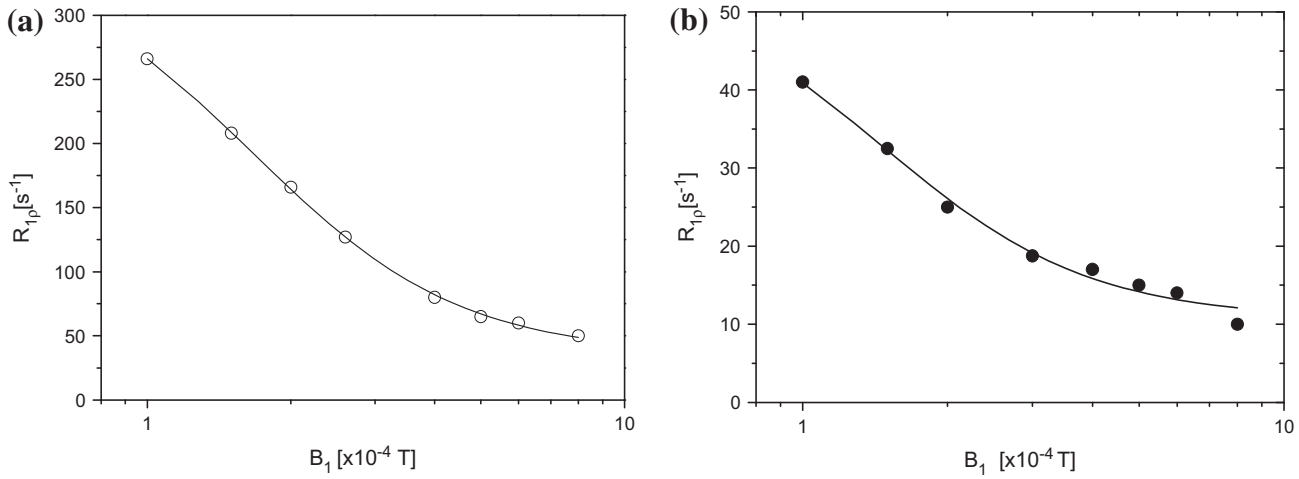

Fig. 5. Fit of the data taken from reference [4] with Eq. (4) for cellulose samples with (a) MC = 49.9% and (b) MC = 218% measured at 25 °C.

Table 1
Values of T_1 and obtained from dispersion profiles for cellulose, starch powders of different origin, paper samples and lyophilized protein powders at room temperature.

Sample		T_1 (ms)	Correlation time (10^{-5} s)
Cellulose	Water suspension (MC above 100%)	1380 ± 20	1.4 ± 0.7
	Cellulose powder (MC = 15%)	460 ± 20 and 20 ± 10	1.9 ± 0.8
Starch	Potato (MC = 13%)	172 ± 1	2.1 ± 0.9
	Corn (MC = 8%)	209 ± 2	3.6 ± 1.9
	Oat (MC = 7%)	195 ± 4	2.2 ± 0.9
	Wheat (MC = 8%)	196 ± 2	2.3 ± 0.9
Paper (MC = 10%)	Type "Swiecie", (specially produced as a paper of long durability)	256 ± 5 and 30 ± 10	46 ± 1
	Modern	155 ± 5	16 ± 1
	Old (1951)	68 ± 1 and 15 ± 7	5. 3 ± 3.5
	Cotton threads	277 ± 10 and 30 ± 10	1.5 ± 0.7
Proteins (MC = 10%)	Albumin	144 ± 2	2.5 ± 1.5
	Lysozyme	173 ± 3	2.8 ± 1.1
	Haemoglobin	35.0 ± 0.3	1.3 ± 0.7

Table 1 presents the correlation times for the lyophilized protein samples: albumin, lysozyme and haemoglobin. Correlation times for albumin and lysozyme powder are very similar. Both T_1 and τ for haemoglobin are distinctly shorter than for albumin and lysozyme. The former is expected to result from presence of proton–paramagnetic ion interaction in haemoglobin. An approach to describe $T_{1\rho}$ dispersion profile in this case is not know at this time and in the presence of other interactions it needs special experimental and theoretical work.

It is of interest to compare the correlation times obtained in the present study to values published in the literature for related systems. Although abundant literature exists on biopolymer systems at high hydration levels (e.g., solutions, suspensions, pastes) the information available on slow dynamical modes of water (in the mid-kilohertz range) in biopolymer powders or solid biopolymer matrices, at above freezing temperatures, is more limited. In addition, literature available in connection with the latter, where correlation times for such slow dynamics of hydration are given, is very limited, making comparisons difficult. The following literature explicitly supplies information regarding the correlation times of the slow water dynamics mode in these systems.

From field cycling dispersion data [22] in albumin powder, with a moisture content of 25%, we estimate a correlation time of 5 μs for the water of hydration. Although the uncertainty in this estimate is not known this value does compare favorably with the value (25 ± 15) μs (Table 1) found in the present study. In a proton NMR study of water in native waxy maize starch (moisture content = 10%) it was found that the water associated with the polysaccharide chains is highly mobile and undergoes anisotropic motion describable through two correlation times [34]. A value of 60 μs was estimated by the authors for the slower of these two correlation times, which essentially agrees, within the experimental uncertainty, with the value of (36 ± 19) μs for corn starch listed in Table 1. The faster of the two correlation times was estimated to be of the order of nanoseconds and is too fast to contribute to the dispersion step in our measurements in corn starch.

In the above discussion and analysis it has been assumed that by monitoring amplitudes on the liquid-like part of the FID it is the water protons that are being studied. Under the right conditions (moisture content, temperature) a part of some polymers can exhibit more liquid-like dynamics due to plasticization effects and the above assumption warrants additional comment. For example, in a ^{1}H and ^{13}C NMR study [35] of wheat starch paste samples it was found that up to 60% of the polymer was relatively mobile. In a sample of moistened (33% moisture content) starch granules, ^{13}C CP/MAS experiments combined with single pulse ^{13}C MAS experiments indicated that ~50% of the starch exhibited liquid-like behavior [31]. The degree to which water would plasticize a polymer depends on the type of polymer involved, the temperature and the moisture content. Both of the above starch systems involve moisture contents considerably higher than for the samples being considered here (except for the cellulose suspension the samples' moisture contents do not exceed 15%, Table 1). The importance of decreased moisture content can be seen from a study of maize starch, at 12% moisture content, which did not exhibit polymer motions in the tens of kilohertz regime [36]. In such a samples a correlation time in the 20–30 μs range, detected in the present study, would not be associated with polymer dynamics. The data for the $T_{1\rho}$ dispersion results reported here were recorded on the liquid part of the FIDs and additional information about possible contributions made by polymer protons to the liquid-like part of the FID in low hydration samples comes from time domain results reported in the literature. A comparison of the proton FID in a lysozyme sample, hydrated to 24% moisture content, to the FID in dry lysozyme indicated that at this hydration level the polymer protons do not contribute to the liquid-like FID [37]. In an absolute moisture content study of wood samples, using proton FID measurements, it was found that as the moisture content was increased from 0% to 15% the liquid-like part of the FID signal acquired an amplitude from mobile polymer protons amounting to a maximum of about 1/10 of the liquid-like FID at the 15% hydration level [38]. A major wood constituent is cellulose and thus this result gives some indication of the plasticization effect in cellulosic material at this low moisture content. Although

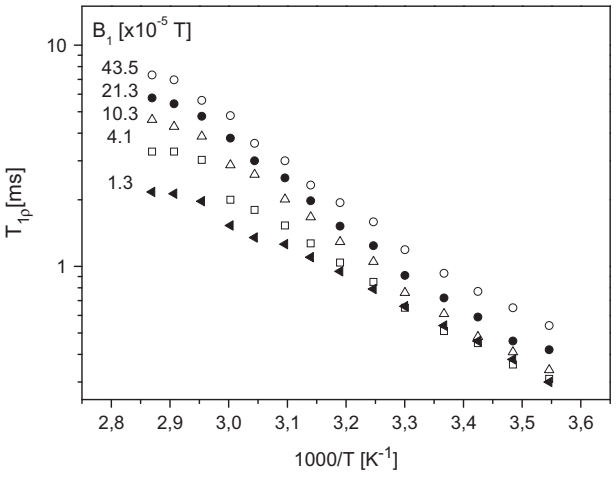

Fig. 6. Temperature dependence of $T_{1\rho}$ for native starch at different B_1 values.

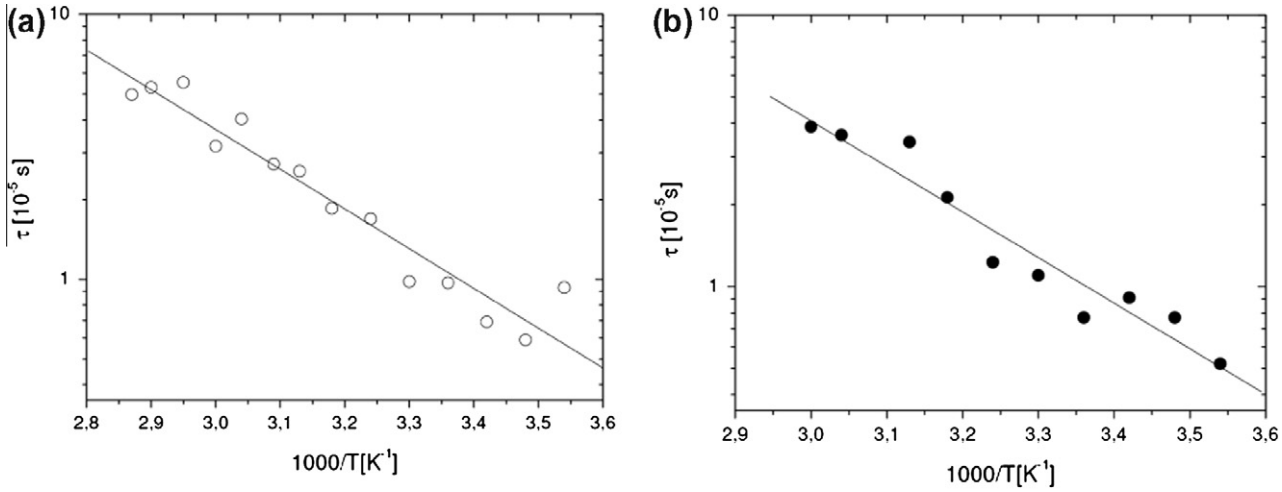

Fig. 7. Temperature dependence of correlation times obtained from dispersion profiles for each temperature for (a) native potato starch and (b) dry-processed potato starch. The solid lines represent Arrhenius plots calculated from Eq. (5).

indications are that in some of the samples studied a part of the signal being measured is due to liquid-like polymeric components such contributions appear small at these low hydration levels and we take the present $T_{1\rho}$ dispersion results to reflect water molecule dynamics.

A second parameter of molecular dynamics, the activation energy, can be calculated from the temperature dependence of the correlation times obtained from the dispersion profiles. Fig. 6 shows the temperature and B_1 dependence of $T_{1\rho}$ for native starch and Fig. 7a shows the temperature dependence of the correlation times obtained from the dispersion profiles. Fig. 7b shows the temperature dependence of τ for dry-processed potato starch. Linear fits of the data in Fig. 7a and b with the function

$$\log \tau = a_1.(1000/T) + a_2 \quad (5)$$

allows us to calculate the activation energy for native and dry-processed potato starch from the obtained parameters a_1. These are: E(native) = 29 ± 3 kJ/mol and E(dried)=32 ± 2 kJ/mol, respectively. The finding that the activation energies for the slow motion, monitored in the $T_{1\rho}$ dispersion experiments, are essentially the same in these different proteins is in keeping with the idea that in general the behavior of water closely associated with the biopolymer does not differ appreciably from one polymer to another. Considering that the hydrogen bond energy is about 15 kJ/mole suggests that perhaps more than a single hydrogen bond needs to break for this water to reorient appreciably.

It is interesting to compare the above activation energy to values found for hydration water in other systems. In a recent NMR study [20] correlation times for water of hydration of myoglobin, elastin and collagen are presented as a function of temperature. An activation energy of about 50 kJ/mol is observed for all three proteins. The correlation times for the three proteins are about the same at a given temperature and equal to about 0.1 ns at $1000/T = 4\ K^{-1}$. In the present study the correlation times have been derived from $T_{1\rho}$ dispersions and characterize different motions than those in [20]. From the temperature dependence of the correlation times in Fig. 7a and b it is seen that at $1000/T = 3.5\ K^{-1}$ the correlation time equals about 5 μs. Although it is not surprising that the activation energies are different for these different motional modes of the water, at the present time it is not known why a smaller activation energy is associated with the slower motional mode.

4. Conclusion

The values of correlation times obtained from $R_{1\rho}$ dispersion profiles are similar to those obtained by other authors [33]. In addition, the values of activation energies found here are in good correspondence with those in related systems reported elsewhere [2,6]. An interesting result is that for a particular polymer the correlation times derived from $R_{1\rho}$ dispersion profiles are not strongly dependent on hydration level. However, values of $T_{1\rho}$ as well as T_1 are strongly controlled by MC. This was interpreted to imply that the slow, local dynamics of interfacial water does not differ much between different polymers and that differences in the amount of water closely associated with the polymer relative to that less associated with the polymer, leads to the large, observed differences in the T_1 values.

References

[1] V.J. McBrierty, K.J. Packer, Nuclear Magnetic Resonance in Solid Polymers, Cambridge University Press, Cambridge, 1993.
[2] K. Banas, B. Blicharska, W. Dietrich, M. Kluza, Molecular dynamics of cellulose–water systems investigated by NMR relaxation method, Holzforschung 54 (2000) 501–504.
[3] H. Ono, H. Yamada, S. Matsuda, K. Okajima, T. Kawamoto, H. Iijima, 1H-NMR relaxation of water molecules in the aqueous microcrystalline cellulose suspension systems and their viscosity, Cellulose 5 (1998) 231–247.
[4] H. Peemoeller, A.R. Sharp, NMR study of cellulose–water systems: water proton spin–lattice relaxation in the rotating reference frame, Polymer 26 (1985) 859–864.
[5] A. Rachocki, J. Kowalczuk, J. Tritt-Goc, How we can interpret the T_1 dispersion of MC, HPMC and HPC polymers above glass temperature?, Solid State Nuclear Magnetic Resonance 30 (2006) 192–197.
[6] A. Rachocki, J. Tritt-Goc, The molecular origin of nuclear magnetic relaxation in methyl cellulose and hydroxypropylmethyl cellulose, Journal of Polymer Research 13 (2006) 201–206.
[7] H.R. Tang, P.S. Belton, Proton relaxation in plant cell walls and model systems, in: P.S.H. Belton, B.P. Webb (Eds.), Advances in Magnetic Resonance in Food Science, Woodhead Publishing Ltd., 1999, pp. 166–184.
[8] H.R. Tang, B.L. Zhao, P.S. Belton, L.H. Sutcliffe, A. Ng, Anomalous proton NMR relaxation behavior of cell wall materials from Chinese water chestnuts, Magnetic Resonance in Chemistry 38 (2000) 765–770.
[9] H.R. Tang, P.S. Belton, A. Ng, K.W. Waldron, P. Ryden, Solid state H-1 NMR studies of cell wall materials of potatoes, Spectrochimica Acta Part A – Molecular and Biomolecular Spectroscopy 55 (1999) 883–894.
[10] S.K. Koskinen, P.T. Niemi, S.A. Kajander, M.E.S. Komu, $T_{1\rho}$ dispersion profile of rat tissues in vitro at very low locking fields, Magnetic Resonance Imaging 24 (2006) 295–299.
[11] L. Calucci, L. Galleschi, M. Geppi, G. Mollica, Structure and dynamics of flour by solid state NMR: effects of hydration and wheat aging, Biomacromolecules 5 (2004) 1536–1544.

[12] M. Ritota, R. Gianferri, R. Bucci, E. Brosio, Proton NMR relaxation study of swelling and gelatinisation process in rice starch–water samples, Food Chemistry 110 (2008) 14–22.
[13] U. Duvvuri, A.D. Goldberg, J.K. Kranz, L. Hoang, R. Reddy, F.W. Wehrli, A.J. Wand, S.W. Englander, J.S. Leigh, Water magnetic relaxation dispersion in biological systems: the contribution of proton exchange and implications for the noninvasive detection of cartilage degradation, Proceedings of the National Academy of Sciences of the United States of America 98 (2001) 12479–12484.
[14] H.I. Makela, O.H.J. Grohn, M.I. Kettunen, R.A. Kauppinen, Proton exchange as a relaxation mechanism for T-1 in the rotating frame in native and immobilized protein solutions, Biochemical and Biophysical Research Communications 289 (2001) 813–818.
[15] S.H. Koenig, R.D. Brown III, U. Raphael, A unified view of relaxation in protein solutions and tissue, including hydration and magnetization transfer, Magnetic Resonance in Medicine 29 (1993) 77–83.
[16] R.T. Engelhardt, G.A. Johnson, T_{1rho} relaxation and its application to MR histology, Magnetic Resonance in Medicine 35 (1996) 781–786.
[17] R.S. Menon, P.S. Allen, Solvent proton relaxation of aqueous solutions of the serum proteins alpha 2-macroglobulin, fibrinogen, and albumin, Biophysical Journal 57 (1990) 389–396.
[18] M.J. Silvennoinen, M.I. Kettunen, C.S. Clingman, R.A. Kauppinen, Blood NMR relaxation in the rotating frame: mechanistic implications, Archives of Biochemistry and Biophysics 405 (2002) 78–86.
[19] S.K. Koskinen, A.M. Virta, P.T. Niemi, S.A. Kajander, M.E.S. Komu, $T_{1\rho}$ dispersion of rat tissues in vitro, Magnetic Resonance Imaging 17 (1999) 1043–1047.
[20] S.A. Lusceac, M.R. Vogel, C.R. Herbers, H-2 and C-13 NMR studies on the temperature-dependent water and protein dynamics in hydrated elastin, Myoglobin and collagen, Biochimica Et Biophysica Acta – Proteins and Proteomics 1804 (2010) 41–48.
[21] J. Andrasko, Water in agarose gels studied by nuclear magnetic-resonance relaxation in rotating frame, Biophysical Journal 15 (1975) 1235–1243.
[22] R. Kimmich, E. Anoardo, Field-cycling NMR relaxometry, Progress in Nuclear Magnetic Resonance Spectroscopy 44 (2004) 257–320.
[23] J.S. Blicharski, Nuclear magnetic relaxation in rotating frame, Acta Physica Polonica A 41 (1972) 223–236.
[24] J.B. Lambert, E.P. Mazzola, Nuclear Magnetic Resonance Spectroscopy: An Introduction to Principles, Applications and Experimental Methods, Pearson Prentice Hall, Upper Saddle River, New Jersey, 2004.
[25] Field Cycling Relaxometry. Review of Technical Issues and Applications, Stelar s.r.l, ver.6/2005.
[26] W.M. Shirley, R.G. Bryant, Proton-nuclear spin relaxation and molecular-dynamics in the lysozyme–water system, Journal of the American Chemical Society 104 (1982) 2910–2918.
[27] H.R. Tang, J. Godward, B. Hills, The distribution of water in native starch granules – a multinuclear NMR study, Carbohydrate Polymers 43 (2000) 375–387.
[28] A. Buleon, P. Colonna, V. Planchot, S. Ball, Starch granules: structure and biosynthesis, International Journal of Biological Macromolecules 23 (1998) 85–112.
[29] A. Buleon, C. Gerard, C. Riekel, R. Vuong, H. Chanzy, Details of the crystalline ultrastructure of C-starch granules revealed by synchrotron microfocus mapping, Macromolecules 31 (1998) 6605–6610.
[30] D.J. Gallant, B. Bouchet, P.M. Baldwin, Microscopy of starch: evidence of a new level of granule organization, Carbohydrate Polymers 32 (1997) 177–191.
[31] K.R. Morgan, R.H. Furneaux, N.G. Larsen, Solid-state NMR-studies on the structure of starch granules, Carbohydrate Research 276 (1995) 387–399.
[32] W.R. Morrison, Starch lipids and how they relate to starch granule structure and functionality, Cereal Foods World 40 (1995) 437–446.
[33] D. Capitani, A.L. Segre, D. Attanasio, B. Blicharska, B. Focher, G. Capretti, 1H NMR relaxation study of paper as a system of cellulose and water, Tappi Journal 79 (1996) 113–122.
[34] S.F. Tanner, B.P. Hills, R. Parker, Interactions of sorbed water with starch studied using proton nuclear magnetic resonance spectroscopy, Journal of the Chemical Society, Faraday Transactions 87 (1991) 2613–2621.
[35] P.T. Callaghan, K.W. Jolley, J. Lelievre, R.B.K. Wong, Nuclear magnetic resonance studies of wheat starch pastes, Journal of Colloid and Interface Science 92 (1983) 332–337.
[36] A.S. Kulik, J.R.C. Decosta, J. Haverkamp, Water organization and molecular mobility in maize starch investigated by 2-dimensional solid-state NMR, Journal of Agricultural and Food Chemistry 42 (1994) 2803–2807.
[37] H. Peemoeller, R.K. Shenoy, M.M. Pintar, Two-dimensional NMR time evolution correlation spectroscopy in wet lysozyme, Journal of Magnetic Resonance 45 (1981) 193–204.
[38] I.D. Hartley, F.A. Kamke, H. Peemoeller, Absolute moisture content determination of aspen wood below the fiber saturation point using pulsed NMR, Holzforschung 48 (1994) 474–479.